Scaling laws in magneto-optical properties of aggregated ferrofluids

R. Botet
Laboratoire de Physique des Solides, CNRS, Bâtiment 510, Université Paris–Sud, Centre d'Orsay, F-91405 Orsay, France

K. N. Trohidou
Institute of Materials Science, National Center for Scientific Research "Demokritos," 15310 Athens, Greece

J. A. Blackman
Department of Physics, University of Reading, Whiteknights, P.O. Box 220, Reading RG6 6AF, United Kingdom

D. Kechrakos
Institute of Materials Science, National Center for Scientific Research "Demokritos," 15310 Athens, Greece
(Received 16 December 2000; revised manuscript received 20 March 2001; published 28 August 2001)

Since statistically isotropic fractal aggregates of particles are a particular case of self-organized critical systems, we describe formally field-induced behaviors of aggregated ferrofluids as responses of regular at-equilibrium critical systems at the critical point to the small field conjugated to its order parameter. This leads us to expect some general scaling laws, which are checked numerically on two examples: the magnetic susceptibility and the magneto-optical linear dichroism of two-dimensional aggregated ferrofluids. This is performed by numerical simulations of such an aggregating system under weak magnetic field applied in the plane of the aggregates.

DOI: 10.1103/PhysRevE.64.031401 PACS number(s): 61.43.Hv, 75.50.Tt, 75.40.Mg, 33.55.Fi

I. INTRODUCTION

A ferrofluid consists of colloidal magnetic particles dispersed in a nonmagnetic liquid carrier [1,2]. Often, these particles are formed well monodispersed and small enough to constitute a single magnetic domain. Their mean diameter is typically adjusted in the range 10–40 nm. Moreover, their global shape does not show any relevant morphological anisotropy and can be approximated by a sphere, even if some crystalline anisotropy can appear in their local magnetic properties [3]. In free space, these particles may aggregate to form complicated shapes such as chains, loops, and branching points [4–6], and their statistical morphology is fractal, with a fractal dimension depending on the magnitude of the magnetic moments of the individual particles. These unusual shapes are difficult to handle analytically, and this explains why little is known theoretically about the equation of state [7]. Hence, numerical simulations represent the standard tool to understand their unique features, and extensive works have been performed to characterize the morphology of the ferrofluid aggregates [8]. Under an external magnetic field, particles are known to aggregate in a way dependent on the field [9,10], with preference for chains in the case of the weak concentrations, and of labyrinthic patterns for the large concentrations.

Even though conceptually simple, these magnetic materials exhibit quite unusual and exciting properties for which complete understanding is yet a challenge. In the present work, we consider the optical response of a thin slab of ferrofluid, with low concentration of magnetic particles, subjected to a constant external magnetic field in the plane of the slab (see Fig. 1).

Such magneto-optical effects are known to be rather important in magnitude, and they are used nowadays to characterize the ferrofluid state [11,12]. To be more precise, we consider here the incident transverse electromagnetic wave with the wave-vector perpendicular to the slab, and we investigate the properties of the transmitted wave. Two polarizations of the electric field have to be discussed: the incident polarization parallel to the magnetic field (the parallel polarization, denoted $||$), and the incident polarization perpendicular to the magnetic field (the perpendicular $\perp$, polarization). Such a system is experimentally known to have important magneto-optical properties, probably due to particular aggregation and collective orientation induced by the field [10,13–15]. In this paper, we discuss more precisely the case of the linear dichroism for simulated aggregates under the magnetic field. In addition, the temperature of the system is assumed to be small enough and low concentration is used, in order to study only the role of the aggregate morphology and orientation.

II. GROWTH SIMULATION ON THE TRIANGULAR LATTICE

The numerical simulation of ferrofluid aggregation is a long story, beginning with the work of Chantrell [16]. Among the various ways to simulate numerically two-dimensional ferrofluid aggregation, it has been shown that simulation on a triangular lattice is convenient [17]. In effect, this kind of simulation is able to reproduce correctly the behavior of clusters generated by more sophisticated ways (e.g., off-lattice Langevin dynamics [18]) but the computing effort is considerably reduced since much of the computations are realized on integer instead of real numbers [17]. Nevertheless, the particular symmetries of the triangular lattice need some care. For example, when an external field is used, this field should by no means be connected to the lat-

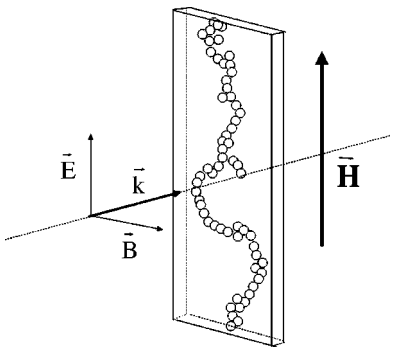

FIG. 1. Schematic view of the system investigated in the present work. The ferrofluid is confined inside a slab, and light [wave vector **k**, and (**E,B**) is the electromagnetic field] arrives perpendicularly to it. A constant magnetic field **H** is set in the plane of the slab. This figure is drawn for the parallel-polarization case (**E** parallel to **H**).

tice (this is a real-component vector), and averaging has to be done to avoid symmetry artifacts.

A system of N identical particles of diameter $d=2a$ is generated randomly at the initial time. Each particle is allowed to stay on node of a triangular lattice of size $L=N$. This is the simplest choice to avoid artificial self-interaction of linear-shaped clusters. At each particle i is attached to a three-dimensional real magnetic moment $\mathbf{m}_i$ of given common modulus m, in order to simulate single-domain ferromagnetic particles. The small temperature of the whole system is homogeneous and set equal to T, and an external magnetic field $\mathbf{H}=H\mathbf{u}_H$ is applied in the two-dimensional plane. The reduced energy of the system is then equal to

$$U/k_BT=K_{mT}\left(\sum_{i\neq j}\left[\mathbf{m}_i\cdot\mathbf{m}_j-3(\mathbf{m}_i\cdot\mathbf{u}_{ij})(\mathbf{m}_k\cdot\mathbf{u}_{ij})\right]/r_{ij}^3 - K_{mH}\sum_i \mathbf{m}_i\cdot\mathbf{u}_H\right). \quad (1)$$

In this expression, the two nondimensional parameters $K_{mT}=m^2/d^3k_BT$ and $K_{mH}=Hd^3/m$ are used. They represent the relative strengths of the moment–moment interaction to the thermal energy, and of the magnetic moment to external field, respectively. Note that we prefer to use here K_{mH} instead of the more usual parameter: $mH/k_BT=K_{mH}K_{mT}$, since the system under investigation is only subjected to small values of the temperature T, so K_{mH} takes reasonable finite values.

The system is stabilized so that electrostatic and van der Waals interactions between particles can be neglected when compared to the magnetic forces. The aggregation scheme is based on the diffusion-limited cluster aggregation process [19,20] developed for short-ranged interaction particle aggregation. When, during their motion, two particles are on neighboring nodes, they stick. In addition, we make the usual assumption that sticking is irreversible due to the small temperature of the system, and absence of any hydrodynamic stress. An isolated particle will be considered as a cluster of size 1. The Metropolis algorithm [21] is used at each Monte Carlo step: a random movement (translation or rotation) of a cluster is assumed. If this move corresponds to a decrease of the system energy, it is performed. If this corresponds to an increase $\Delta U>0$ of this energy, it is performed with the probability $\exp(-\Delta U/k_BT)$. After each tentative movement, relaxation of all the magnetic moments is performed: if $\mathbf{H}_i$ represents the local apparent field applied on the particle i, its magnetic moment is aligned along this field. In principle, this alignment should not be perfect and modelized, for example, according to the Metropolis algorithm with the local energy $-\mathbf{m}_i\cdot\mathbf{H}_i$, but here the temperature is chosen such that this approximation of perfect alignment holds. This sequence of process is repeated until an equilibrium configuration is found for the whole system.

We do not consider here the fractal morphology of such aggregates as a function of the applied field. This aspect has been studied in detail elsewhere [22,8]. Three typical aggregates of $N=64$ particles, formed at different values of K_{mH}, are shown in Fig. 2.

III. CALCULATION OF THE OPTICAL PROPERTIES

To compute the optical properties of such aggregates, we suppose that the radius of the particles is so small that each of them can be replaced by a single electromagnetic dipole. This is the case for scatterers of radius of some nanometers, interacting with light. One defines then the Clausius–Mossotti dielectric susceptibility [23] $\chi_p=(3/4\pi)[(n_p^2-n_1^2)/(n_p^2+2n_1^2)]$, and the polarizability [24] $\alpha_p=v_p\chi_p$ for each particle of volume v_p and refractive index n_p. We treat here the simple case where the scattering particles are not at an optical resonance, in order to avoid problems of light localization [25]. The refractive index n_1 is for the dispersing nonmagnetic medium. The electromagnetic dipole moment $\mathbf{P}_i$ of particle i is then the product of its polarizability and of the *total* local electric field. More precisely, the set of self-consistent linear equations is

$$\mathbf{P}_i=\alpha_p\left(\mathbf{E}_{\rm inc}+\sum_{j\neq i}\hat{G}(r_{ij})\mathbf{P}_j\right), \quad (2)$$

where the free-space Green tensor is given by

$$\hat{G}(\mathbf{r})=k^3(A(kr)\delta_{\alpha\beta}-B(kr)u_\alpha u_\beta).$$

In the latter expression, the functions A and B are [26] $A(x)=(x^{-1}+ix^{-2}-x^{-3})\exp(ix)$, $B(x)=(x^{-1}+3ix^{-2}-3x^{-3})\exp(ix)$, and $\delta_{\alpha\beta}$ is the Kronecker symbol applied to the two Cartesian coordinates α and β. This constitutes the basic discrete dipolar approximation equations [27,28], in the case of one electromagnetic dipole per particle. The equation (2) can be rewritten introducing the discrete polarization distribution $\mathbf{d}_i=\mathbf{P}_i/v_p$, and the tensor of effective optical susceptibility $\hat{\chi}_i$, as

$$\mathbf{d}_i=\chi_p\left(\mathbf{E}_{\rm inc}+\sum_{j\neq i}v_p\hat{G}(r_{ij})\mathbf{d}_j\right)=\hat{\chi}_i\mathbf{E}_{\rm inc}. \quad (3)$$

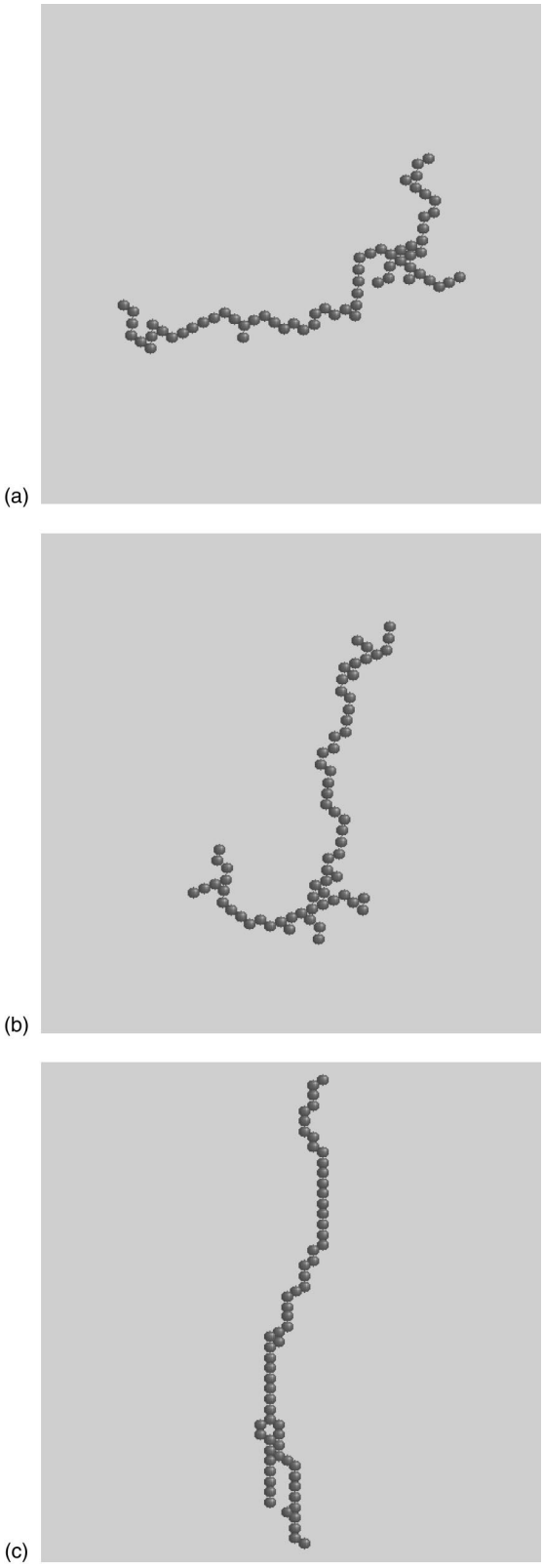

FIG. 2. Three aggregates of 64 monodisperse particles on a two-dimensional triangular lattice, with density about 1%. The values of K_{mH} are (a) 0, (b) 0.05, and (c) 0.5, and $K_{mT}=10\,000$. The direction of the magnetic field is from the bottom to the top of the page of the diagram.

We see that if one knows the solution of Eq. (3), then the susceptibility tensor of each particle can be calculated, and the average value $\langle\hat{\chi}\rangle$ estimated for one aggregate. These equations are solved by the efficient scattering-order method [29]: inversion of the linear Eq. (3) is formally expressed as a series of terms corresponding, respectively, to the successive scattering orders (the first term is the incident field, the second is the single-scattering field, and so on). Each higher-order field is calculated using the previous-order field, until series convergence is achieved.

We consider now a monodisperse collection of aggregates of size N, all formed in the same physical conditions, and ν will denote the volume concentration of the system. An electromagnetic plane wave propagating inside this medium will have an oscillating electric field **E** solution of the wave equation:

$$\boldsymbol{\nabla}\times\boldsymbol{\nabla}\times\mathbf{E}+\frac{n_1^2}{c^2}\frac{\partial^2\mathbf{E}}{\partial t^2}=-\mu_o\nu P(\mathbf{d}\rangle$$

with $\langle\mathbf{d}\rangle$ the average discrete polarization distribution for *one* particle of the system. Taking the Fourier transform allows us to express the dispersion equation for the monochromatic wave as a function of the average susceptibility tensor of one particle [30,31]:

$$n^2=n_1^2(1+\nu\langle\hat{\chi}\rangle)\,. \tag{4}$$

We have supposed that the electromagnetic wave does not interact with the static magnetic moments of the particles, induced by the external magnetic field, such that the effective refractive index for the system reflects only the geometrical arrangement of the particles. Of course, averaging over a large number of independent aggregates is needed to achieve an accurate estimate of the refractive index of the system.

IV. MAGNETIZATION

In the absence of external magnetic field, the morphology of aggregates of ferromagnetic particles is fractal, and characterized by the fractal dimension $D_f=1.23$ [32,17], for large magnetic moments per particle. The dipolar magnetostatic interaction depending on both long-range and directional particle correlations, the average magnetization per particle, $M=|(1/N)\Sigma_i\mathbf{m}_i|$, reflects these particular long-ranged fractal correlations [33]. It should result in a broad distribution of the local fields (due to all the dipoles) inside the aggregate. As a consequence, the effectiveness of the external field H, in aligning a magnetic moment will vary from position to position according to the strength of the local field, and one can anticipate that the function M vs H, expected to be linear in the case of short-range interactions, should not be so simple in the present case. Experimentally, this function is known to have a gigantic slope at the zero field.

We can guess a generic form for the magnetization in small external fields with the following argument. Correlation functions of fractal objects decrease as power laws. Such zero-field ferrofluid aggregates can then be considered as

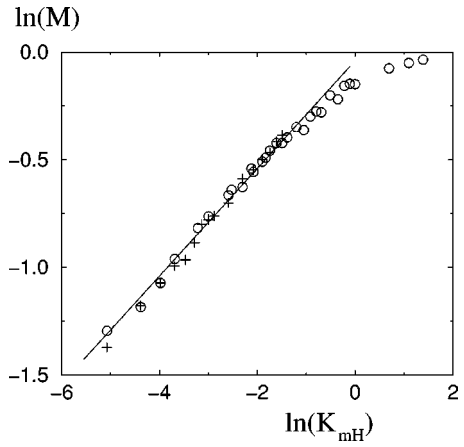

FIG. 3. Double-logarithmic plot of the magnetization of two-dimensional aggregates of size $N=32$ (crosses) and $N=64$ (circles) as a function of the reduced in-plane magnetic field K_{mH}. The magnetization at saturation is denoted M_0, and is equal to 1 with our units. Each point is the average over 2000 and 1000 independent clusters, respectively. The behavior for small values of the field is a power law with exponent 0.23 ± 0.02, as shown by the line, followed by the saturation $M/M_0=1$ for the high fields.

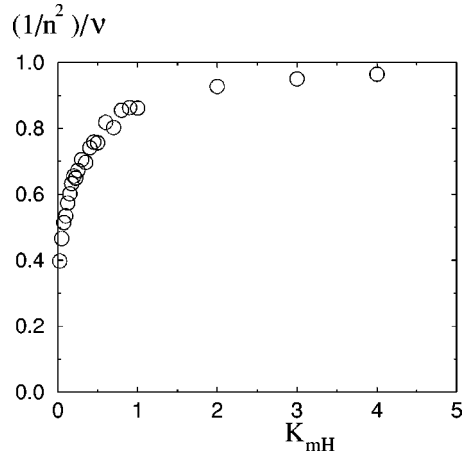

FIG. 4. Plot of the imaginary part of $\Delta(1/n^2)/\nu$ *vs* in-plane applied magnetic field K_{mH}, for 1000 two-dimensional aggregates of size $N=64$.

self-organized critical systems [34], since this criticality arises here without tuning of the driving parameters [35]. Another point which goes with the critical behavior of such objects, is the *M*-finite-size scaling demonstrated numerically in these kind of ferrofluid aggregates [36]: $|M_N-M_\infty| \sim N^{-1/D_f}$. Hence, applying a small external field to such a structure is equivalent to applying this field to a critical magnetic system *at the critical point*. One can then expect the magnetization to be of the form $M\sim H^{1/\delta}$, with a value of the critical exponent δ larger than 1, and probably quite large. We have in principle to shift the results by the zero-field magnetization (but this correction is small as compared to the magnetization under field), according to the complete formula $M_N(H)-M_N(0)\sim H^{1/\delta}$. In Fig. 3 is one example for $N=64$ and $N=32$ aggregates at small volume concentration (1% and 2%, respectively).

This power-law behavior is clear when the external field is not large enough to saturate the magnetization. Here we find an exponent 0.23 ± 0.02, corresponding to a value $\delta=4.4\pm0.4$, amazingly very close to the usual values of this critical exponent for a number of second-order magnetic phase transitions. Note also that it is definitely not equal to the value $\delta=3$ derived for the mean-field theory. The behavior of the magnetization is clearly not linear with the magnetic field, and gives a diverging magnetic susceptibility in the zero field. The same kind of analysis, with the same results and same exponents, can be done for the modulus of the averaged projection of **M** on the magnetic field **H**. Since, by symmetry, this averaged projection is zero for zero field this quantity acts just as an order parameter for the system, with the external field as its conjugated field.

V. LINEAR DICHROISM

Linear dichroism occurs when the imaginary part of the refractive index depends on the state of polarization of the incident wave. This is the case, in particular, for magneto-optical dichroism of ferrofluid [37] in the applied magnetic field. Two directions for the polarization are then to be studied: when polarization is parallel to the applied field, or when it is perpendicular to it. Generally, the difference between the refractive indices is scaled by volume concentration in order to eliminate trivial linear (for small densities) concentration dependence. In the following calculations, we assumed that the magnetic particles are homogeneously constituted of Fe_3O_4, with complex refractive index $n_p=2.2-i$ 0.58, in water (refractive index $n_1=1.33$) [13]. Each particle is a sphere of radius $a=4$ nm, and the incident electromagnetic wave has a wavelength $\lambda=633$ nm. We explained above (in Sec. III) how to compute the complex refractive index n of the slab. In principle, it could be a full 2×2 tensor, after Eq.(4), but it is found to be almost diagonal for any physical conditions we studied (off-diagonal terms are found to be about 10^{-3} times the diagonal terms in all our simulations). So, we used only the two diagonal terms to describe the optical properties of the slab for the $\|$ and $\perp$ incident polarizations.

Often, the quantity to measure is set equal to the difference of $1/n^2$ instead of the difference of the refractive indices. We take this convention here, but both forms give readily the same result, since Δn is generally quite small. Figure 4 shows the result of the parameter: $\Delta(1/n^2)/\nu$, re scaled by the volume concentration ν, as a function of the field parameter K_{mH}. After a steep increase, one can see the saturation due to perfect alignment of rodlike aggregates in the field. This behavior is qualitatively the same as measured in the experiments [31].

We should like to discuss now these results in more details. Since there is lack of analytical fit for this kind of curve, precise agreement with the experiments is not so easy to trust, especially because some adjustable parameters must be handled. So, we propose below a scaling formula for the small-field behavior, which is the most interesting case.

The Cotton–Mouton effect is a particular case of magneto-induced orientational linear dichroism appearing in systems of *nonaggregated* magnetic colloidal particles. A

classical formula gives the small-field difference of refractive index between the two incident $\|$ and $\perp$ polarizations, under the form [38]

$$\Delta(1/n^2)/\nu \propto H^2. \tag{5}$$

But this formula must be understood as the consequence of two independent behaviors: the variation of $\Delta(1/n^2)$ with the magnetization per particle, and the dependence of this magnetization with the magnetic field. Let us be more precise with this classical case: the magnetization M of each individual colloidal particle is given by the Langevin function $L(x)=\coth(x)-1/x$, for $x=mH/k_BT$. In particular, for the small magnetic fields H, the magnetization is linear with the field,

$$M \propto H \tag{6}$$

and parallel to it, leading to finite magnetic susceptibility. The Cotton–Mouton formula (5) can then be written as well with this magnetization per particle instead of the magnetic field.

$$\Delta(1/n^2)/\nu \propto M^2. \tag{7}$$

The latter equation is more pertinent than (5) in this context, since it connects $\Delta(1/n^2)/\nu$ to the magnetization per particle, which is directly responsible via the dipolar interaction, for the alignment of the particles, hence for magneto-optical dichroism. But (5) is indeed more interesting for applications since it connects two quantities easily measurable.

Let us consider now the case of *aggregated* ferrofluid. As it has been argued in the preceding section, we expect the relation (6) to hold with an exponent different from 1:

$$M \sim H^{1/\delta} \tag{8}$$

with $\delta=4.4\pm0.4$. But Eq. (7) should change too, since it is essentially a consequence of the particular magnitude *and* the orientation of the magnetization per particle. In the case of aggregated ferrofluids, we have to take account of the collective orientation of the individual magnetic moment inside the aggregate. For example, in one branch of such aggregate, these moments tend to align head-to-tail, and so they follow more or less the geometric shape of the branch, at least for the small external fields. Because the branches point in any direction and not only in the direction of the field, the magnitude of the aggregate magnetization could result in a less pronounced effect of the dichroism. If we follow the idea of the critical phenomenon, we deduce that the difference of refractive index Δn between $\|$ and $\perp$ incident polarizations, being positive only for nonvanishing applied field, should be a singular quantity. Hence, we can assume Δn to behave as a power law of the order parameter (M), like for any singular quantity at the critical point

$$\Delta(1/n^2)/\nu \propto M^{D_m}. \tag{9}$$

This is the relation corresponding to (7) in the case of aggregated ferrofluid, and it is expected to be valid for the small M, with some positive exponent D_m.

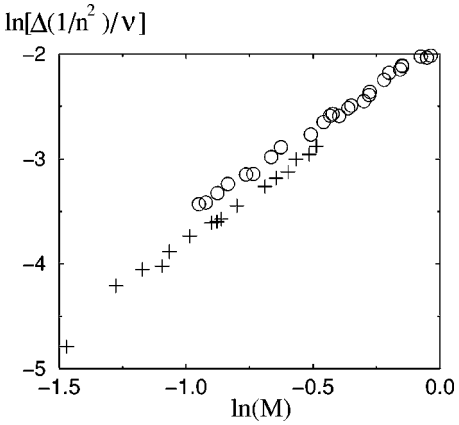

FIG. 5. Double-logarithmic plot of the imaginary part of $\Delta(1/n^2)/\nu$ vs the average magnetization per particle for two-dimensional aggregates of size $N=32$ (crosses) and $N=64$ (circles), when in-plane magnetic field is applied. For each point, 2000 and 1000 independent aggregates are used, respectively, for average. In this figure, magnetization has not been scaled by any N-dependent factor in order to show that this plot could give direct information about the typical size of the aggregates in the system.

We have checked formula (9) with numerical simulations, and one typical result is shown in Fig. 5. The value of D_m is found equal to 1.60 ± 0.05 within an amazingly large range of values of M. It is definitely different from the value 2, expected to hold for small compact particles.

Both results (8) and (9) can be combined to quantify the relation between the difference in the imaginary parts of the refractive index, and the applied magnetic field:

$$\Delta(1/n^2)/\nu \propto H^{D_m/\delta}.$$

From our simulations, we find $D_m/\delta=0.36\pm0.04$, a value very different from the classical value: 2, holding for nonaggregated colloidal particles.

VI. CONCLUSION

In this work we have studied the magnetization and linear dichroism in models of low-density ferrofluids aggregated in a weak magnetic field. The field dependence of both properties exhibit scaling behavior characterized by nontrivial power laws, reminiscent of the critical phenomena, and which originates from the fractal morphology of the clusters and the long-ranged nature of the dipolar interactions. This observation provides new formulas for this kind of magnetic material. Additionally, from a more fundamental point of view, the definition of the exponents δ and D_m could be as important for these systems as the definition of the fractal dimensionality for fractal growth models, and provide a means of characterizing different classes of ferrofluid systems.

ACKNOWLEDGMENTS

This research was supported by Marie-Curie Fellowship Program No. HPMF-CT-1999-00351. R.B. thanks National Center for Scientific Research 'Demokritos' for hospitality during preparation of this work.

[1] S. W. Charles, in *Studies of Magnetic Properties of Fine Particles and their Relevance to Material Science*, edited by J. L. Dorman and D. Fiorani (Elsevier Science, Amsterdam, 1992).
[2] E. Blums, R. Ozols, and R. E. Rosensweig, J. Magn. Magn. Mater. **85**, 303 (1990).
[3] C. H. Griffiths, M. P. O'Horo, and T. W. Smith, J. Appl. Phys. **50**, 7108 (1979).
[4] C. F. Hayes, J. Colloid Interface Sci. **52**, 239 (1975).
[5] J. J. Weis, D. Levesque, and G. J. Zarragoicoechea, Phys. Rev. Lett. **69**, 913 (1992).
[6] P. J. Camp and G. N. Patey, Phys. Rev. E **62**, 5403 (2000).
[7] S. Banerjee, R. B. Griffiths, and M. Widom, J. Stat. Phys. **93**, 109 (1998).
[8] P. Meakin and A. T. Skjeltorp, Adv. Phys. **42**, 1 (1993).
[9] P. Hess and P. Parker, Jr., J. Appl. Polym. Sci. **10**, 1915 (1966).
[10] A. Martinet, Rheol. Acta **13**, 260 (1974).
[11] S. Wilson, P. J. Ridler, and B. R. Jennings, J. Phys. D **29**, 885 (1996).
[12] J.-C. Bacri, R. Perzynski, D. Salin, and J. Servais, J. Phys. (Paris) **48**, 1385 (1987).
[13] P. C. Scholten, IEEE Trans. Magn. **16**, 221 (1980).
[14] Yu. N. Skibin, V. V. Chekanov, and Yu. L. Raikher, Sov. Phys. JETP **45**, 496 (1977).
[15] S. Taketomi, Jpn. J. Appl. Phys. **22**, 1137 (1983).
[16] R. W. Chantrell, A. Bradbury, J. Popplewell, and S. W. Charles, J. Phys. A **13**, L119 (1980).
[17] K. N. Trohidou and J. A. Blackman, Phys. Rev. B **51**, 11521 (1995).
[18] H. Morimoto and T. Maekawa, J. Phys. A **33**, 247 (2000).
[19] P. Meakin, in *Phase Transitions and Critical Phenomena*, edited by C. Domb and J. L. Lebowitz (Academic, New York, 1988), Vol. 12.
[20] R. Botet and R. Jullien, Phase Transitions **24**, 691 (1990).
[21] N. Metropolis, A. W. Rosenbluth, M. N. Rosenbluth, A. H. Teller, and E. Teller, J. Chem. Phys. **21**, 1078 (1953).
[22] P. M. Mors, R. Botet, and R. Jullien, J. Phys. A **20**, L975 (1987).
[23] J. D. Jackson, *Classical Electrodynamics* (Wiley, New York, 1975).
[24] We neglect the radiative-reaction corrections as it should for small and/or absorbing particles, cf. B. T. Draine and J. Goodman, Astrophys. J. **405**, 685 (1993).
[25] D. P. Tsai, J. Kovacs, Z. Wang, M. Moskovits, V. M. Shalaev, J. S. Suh, and R. Botet, Phys. Rev. Lett. **72**, 4149 (1994); V. M. Shalaev, Phys. Rep. **272**, 61 (1996), and references therein.
[26] J. A. Stratton, *Electromagnetic Theory* (McGraw-Hill, New York, 1941).
[27] E. M. Purcell and C. R. Pennypacker, **186**, 705 (1973).
[28] B. T. Draine, Astrophys. J. **333**, 848 (1988).
[29] S. B. Singham and C. F. Bohren, J. Opt. Soc. Am. **5**, 1867 (1988).
[30] H. W. Davies and J. P. Llewellyn, J. Phys. D **13**, 2327 (1980).
[31] M. Xu and P. J. Ridler, J. Appl. Phys. **82**, 326 (1997).
[32] G. Helgesen, A. T. Skjeltorp, P. M. Mors, R. Botet, and R. Jullien, Phys. Rev. Lett. **61**, 1736 (1988).
[33] A. B. Eriksson and M. Jonson, Phys. Rev. B **40**, 884 (1989).
[34] P. Alstrøm, P. Trunfio, and H. E. Stanley, in *Random Fluctuations and Pattern Growth: Experiments and Models*, edited by H. E. Stanley and N. Ostrowski, Vol. 157 of NATO Advanced Studies Institute, Series E (Kluwer, Dordrecht, The Netherlands, 1988), pp. 340-342.
[35] P. Bak and K. Chen, Physica D **38**, 5 (1989).
[36] K. N. Trohidou and D. Kechrakos, J. Phys. C **10**, L255 (1998).
[37] L. Sakhnini and J. Popplewell, J. Magn. Magn. Mater. **122**, 142 (1993).
[38] L. D. Landau, L. P. Pitaevskii, and E. M. Lifshitz, *Electrodynamics of Continuous Media* (Pergamon, Oxford, 1984).